Remote Sensing Applications: Society and Environment 36 (2024) 101363

Contents lists available at ScienceDirect

Remote Sensing Applications: Society and Environment

journal homepage: www.elsevier.com/locate/rsase

A new algorithm to determine the spatial coverage of carob (*Neltuma piurensis*) by ecological floor: Chira-Piura River Basin case

Cristhian Aldana [a], Jaime Lloret [b, *], Wilmer Moncada [c], Joel Rojas Acuña [d], Yesenia Saavedra [a], Vicente Amirpasha Tirado-Kulieva [a]

[a] *Instituto de Investigación para el Desarrollo Sostenible y Cambio Climático INDESC, Universidad Nacional de Frontera, Av. San Hilarión 101, Sullana, 20103, Peru*

[b] *Instituto de Investigación para la Gestión Integrada de Zonas Costeras, Universitat Politecnica de Valencia, C/Paranimf, 1, 46730, Grao de Gandia, Valencia, Spain*

[c] *Laboratorio de Teledetección y Energías Renovables LABTELER, Universidad Nacional de San Cristóbal de Huamanga, Ayacucho, Peru*

[d] *Laboratorio de Teledetección LABTEL, Universidad Nacional Mayor de San Marcos, Lima, Peru*

ARTICLE INFO

Keywords:
Neltuma piurensis
Carob tree
Sentinel 2
Spectral signature
Ecological floor
Chira-piura river basin

ABSTRACT

The carob tree (*Neltuma piurensis*) is characteristic of the forests of northern Peru, withstand extreme climatic events such as "El Niño" and droughts, in addition to the influence of climate change, affecting its distribution of coverage at different altitudes. The objective of this article is to propose an algorithm to determine the Spatial Coverage of Carob by Ecological Floor (SCCEF) in the Chira-Piura River Basin, Peru. The method used consisted of measuring the spectral signature of the carob tree with the FieldSpec4 spectroradiometer at three sampling points corresponding to the localities of Cardal, Lancones and Macacará, located on different ecological floors. The comparison of the spectral signatures for Cardal and Lancones gives an $R^2 = 0.9459$, for Cardal and Macacará an $R^2 = 0.9866$ and for Lancones with Macacará an $R^2 = 0.9469$, which allows an accurate identification of the carob tree in the satellite images. The Mann-Whitney-Wilcoxon *U* test validates the spectral signatures extracted from the satellite images with the spectral signatures measured with the spectroradiometer at Lancones (p-value = 0.9705 $>\alpha = 0.05$), Cardal (p-value = 0.9819 > 0.05) and Macacará (p-value = 0.7959 > 0.05). The results show that the SCCEF in the Tropical (T) ecological floor represents 1.55 % of the T area, in the Tropical Pre-Montane (TPM) ecological floor it is 1.47 % of the TPM area, in the Low Tropical Montane (LTM) ecological floor it is 0.78 % of the LTM area, in the Montane (M) ecological floor it is 0.69 % of the M area and in the Paramo (P) ecological floor it is 0.35 % of the P area. Therefore, the SCCEF decreases in each ecological floor as its altitude increases.

1. Introduction

The vegetation cover in the Chira-Piura River Basin is strongly influenced by extreme climatic events such as droughts and the ENSO (El Niño-Southern Oscillation) event, which is an important factor in the regeneration processes of seasonally dry forests (Holmgren et al., 2006; Richter and Ise, 2005). Many of the extreme climatic events have been dated through dendrochronological studies carried out on the northwest coast of Peru (5° S, 80° W) where ENSO signals have been identified through short ring-width

* Corresponding author.
E-mail addresses: caldana@unf.edu.pe (C. Aldana), jlloret@dcom.upv.es (J. Lloret), wilmer.moncada@unsch.edu.pe (W. Moncada), jrojasa@unmsm.edu.pe (J. Rojas Acuña), ysaavedra@unf.edu.pe (Y. Saavedra), vamir0803@gmail.com (V.A. Tirado-Kulieva).

https://doi.org/10.1016/j.rsase.2024.101363
Received 7 August 2024; Received in revised form 13 September 2024; Accepted 19 September 2024
Available online 20 September 2024

chronologies of Palo Santo (*Bursera graveolens*) during the last 50 years with good correlations for different locations (Rodríguez et al., 2005a).

Likewise, the carob tree (*Neltuma piurensis*), formerly *Prosopis pallida* (Hughes et al., 2022), has in its rings that compose the trunk of the carob tree, chronological information that correlates very well with ENSO events, constructing a master chronology for northern Peru and some physiological derivations from the anatomy of carob tree (López et al., 2005). Preliminary isotopic studies on carob trees also show evidence of ENSO from 1997 to 1998, establishing a strong effect on the variability in the growth of plant species, with positive repercussions on the economy of rural communities for edible and medicinal uses, with wood being the most widely used in housing, cooking, furniture, tools, fodder and the industrialization of some fruits (Rodríguez et al., 2005a).

The "Algarrobo Project" is the most recent proposal, which has allowed the generation of forest cover maps for the departments of Lambayeque, Piura and Tumbes in northern Peru (INRENA Mapa de bosques secos, 2003). In this way, it has been possible to identify the presence of carob trees in most of the areas with dry forest spatial cover in the north of Peru at different altitudinal levels and that according to (La Torre-et al., 2008), a great diversity of plant species characteristic of dry forests can also be observed, such as the sapote (*Capparis scabrida*), the overo (*Cordia lutea*), the ceibo (*Ceiba trischistandra*), the faique (*Acacia macracantha*) and, to a lesser extent, the guayabito de los gentiles (*Capparis avicennifolia*), among others, which accompany the carob tree and are distributed at different ecological levels.

The spatial distribution of carob trees in dry forests plays a very important role in the soil, as they are considered to be nitrogen-fixing, deep-rooted trees that also produce sweet pods that are industrialised as a natural source of energy, as well as being consumed by different types of livestock in some semi-arid grazing areas (Marmillon, 1986).

The potential of the carob tree according to its location by ecological floor is determined from the estimation of its aerial biomass by using destructive methods (17 trees with diameters at the base between 12 and 48 cm), which with the application of allometric equations between the dasometric variables of the carob trees and their biomasses, results in very high correlations between the fresh woody aerial biomass and the dry woody aerial biomass, with respect to the diameters at the base of the tree (Padrón et al., 2004a).

In this sense, 5 ecological floors are defined, determined from the distribution of altitude and biodiversity developed in the different spaces interrelated with climatic and geographical factors corresponding to 31 Life Zones, detailed in the descriptive memory of the Life Zones in the Piura Region (Guerra, 2010). In this way, with the use of the carob tree spectral signature, it will be possible to identify the pixels in the Sentinel 2 images that contain a determined area of carob trees, allowing the estimation of the Spatial Coverage of Carob by Ecological Floor (SCCEF) in the Chira-Piura River Basin of the Piura Region (Aldana et al., 2020).

On the other hand, there are methodologies that use functional traits of carob leaves to show Intraspecific Variability in different ecological zones, where relative variance decomposition shows that leaf structure is highly variable at the population and altitude level, making the carob population varies significantly according to the climatic characteristics of each ecological zone (Salazar et al., 2018), verifying that gas exchange variations are higher at plot level and stomatal variation with variations in leaf chemistry are higher at tree level (Bongers et al., 2017).

For this reason, a deep understanding of the adaptations of the traits of carob leaves in the dry forest is required, because it is a species highly adapted to extremely dry and wet conditions, as it has managed over time to avoid water stress during drought and maximize its growth during ENSO.

Also, in a climate change scenario it could become a key species to understand the resilience of some species and varieties of plants to extreme events in dryland ecosystems (Salazar et al., 2021a). In this sense, the interaction of high temperatures in dry forest ecosystems with water deficit ultimately affects the photosynthesis response in carob trees to a greater extent than the stress of each individual, so that the interactive effect is more pronounced in carob than in other dry forest plant species (Delatorre et al., 2008).

Indeed, there is a need to estimate the SCCEF of the Chira-Piura River Basin using Sentinel 2 satellite images (Borrás et al., 2017), with the application of the spectral signature of the carob tree, for its classification and modelling of the spectral response according to the reflectance value for each wavelength corresponding to 10 of the 13 bands of the Sentinel 2 image (Chávez et al., 2013).

It should be noted that the main objective of this research was to propose a new algorithm to determine the SCCEF in the Chira-Piura River Basin, for which two specific objectives were formulated: to evaluate the SCCEF with the use of Sentinel 2 satellite images in the Chira-Piura River Basin; as well as, to validate the SCCEF with spectral signatures measured with the FieldSpec4 spectroradiometer.

The rest of the paper is structured as follows. Section 2 includes Materials and methods used to perform our research. Section 3 validates the spectral signature of carob from the Sentinel 2 images with the spectral signatures measured with the FieldSpec4 spectroradiometer and calculates the spatial coverage of carob in the 5 ecological floors. Section 4 discusses the results obtained using our algorithm. Section 5 concludes that the spatial coverage of carob decreases in each ecological floor as its altitude increases, and includes our future work.

It is important to take into account that the proposed algorithm is subject to improvement, that means that if the sampling zones for the collection of spectral signatures of carob trees in different locations are increased, then it would contribute to consolidate the validation of both the spectral signatures of the carob tree collected with the spectroradiometer, in relation to the identification of the spectral signatures of the pixels in the Sentinel 2 images.

Likewise, the proposed algorithm has been validated for the carob tree species found in the areas sampled at different altitudinal levels in the Chira-Piura River Basin in Piura-Peru. This means that if we have the spectral signature of any other carob variety worldwide, the algorithm should work when applied to the great diversity of plant species in other ecosystems, which would allow building a big data of spectral libraries that would contribute to an early monitoring system of vegetation cover variation in any geographic region of the world.

It should also be noted that the SNAP software (Sentinel Application Platform, https://earth.esa.int/eogateway/tools/snap, https://step.esa.int/main/download/snap-download/) was used for preprocessing Sentinel 2 images, and ENVI (Image analysis software, https://www.nv5geospatialsoftware.com/Products/ENVI) or QGIS (Quantum GIS, Quantum Geographic Information System, https://www.qgis.org/) or Python (Python Software Foundation, https://www.python.org/) can be used for image processing.

Finally, the application possibilities of this methodological proposal are wide, in such a way that it is possible to apply it in other geographical areas worldwide (this proposal was applied in the Peruvian Andes, as well as in the northern coastal zone of Peru). In addition to this, carob is found in geographical areas of southern Europe, northern Africa, parts of Asia, Spain, the Orient, South America and other countries. Thus, as the carob is an endemic species in the northern coast of Peru, a fundamental part of the dry forest ecosystem in this region of the world, it is important to sustainably monitor their vegetation cover, since the carob both in its fruit and wood has important attributes such as its high nutritional value and extensive durability respectively. It should be noted that the *Neltuma piurensis* has a deep root system, pivotal and vigorous that contributes to some extent to mitigate wind and water erosion.

2. Materials and methods

2.1. Study area

From an ecological and environmental point of view, the methodology was applied to the study of a representative sample area of the dry forest ecosystem where the carob tree (*Neltuma piurensis*) grows; since many of the ecosystem services of the Piura region are a product of this plant species.

On the other hand, given the estimated loss of 22798 ha of dry forest between 2019 and 2021 in Peru, as a case study, the proposed methodology was applied in the geographical area of one of the main tributaries of the region known as the Chira-Piura River, which rises in the western mountain range of the Andes at more than 3000 masl with the name of Catamayo.

The Chira-Piura River basin in the Piura Region is part of the Catamayo-Chira basin shared with Ecuador. The area belonging to Peru is shared with the provinces of Paita, Sullana and Ayabaca. Geographically, it is located between parallels 03°40′28″ and 05°07′06″ south latitude, and meridians 80°46′11″ and 79°07′52″ west longitude.

To the north it borders with the Puyango River Basin, to the south with the Piura and Huancabamba River Basins, to the east with the Zamora and Chinchipe Basins (Ecuador), and to the west, with the Pacific Ocean. It has a surface area of 10615.89 km^2 and a perimeter of 986.401 km, reaching a maximum altitude of 3891 masl.

Then, the Chira River runs 150 km and joins the Macará River where it takes the name of Chira-Piura River, and then runs 50 km serving as a boundary between Peru and Ecuador until it meets the Alamor River. In Peruvian territory it follows a south-westerly direction for approximately 300 km, near the old mouth, until it flows into the sea.

Its climate is dry and arid with the influence of the Humboldt current and the El Niño current on the Peruvian and Ecuadorian coasts. From 0 to 80 masl, rainfall varies from 10 to 80 mm per year between January and April, from 80 to 500 masl it varies from 100 to 600 mm per year between December and May, being dry in the remaining months of the year, with maximum floods occurring during El Niño when accumulated rainfall reaches 2500 mm.

The temporal variation due to evaporation is 6 mm/day and the average air temperature is 26 °C (Varona, 2018). According to National Service of Meteorology and Hydrology of Peru (SENAMHI, in Spanish), anomalous summer temperatures vary from 36 to 40 °C.

Fig. 1 shows the geographical location of the Chira-Piura River Basin and the distribution of the 5 ecological floors in the Chira River Basin, classified according to a Digital Elevation Model (DEM) according to the altitude range (Guerra, 2010).

2.2. Classification of carob tree spatial coverage in sentinel 2 images

The proposed method requires the download of Sentinel 2 satellite images from the Copernicus Open Access Hub server of the European Space Agency (ESA) (European Space Agency Sentinel).

For the mapping of the Chira River Basin, the tiles 20190731T17MPR, 20190830T17MPQ, 20190922T17MNR, 20191029T17MNQ, 20191101T17MNQ, 20191223T17MNR, 20191226T17MMQ are downloaded (Aldana et al., 2020).

Radiometric and atmospheric correction and mosaic tile stitching are performed with the SNAP software (Sentinel Application Platform) (European Space Agency Sentinel), which is an open-source toolbox for reading, preprocessing, analysis and visualisation of Sentinel images.

During pre-processing, radiometric and atmospheric correction is performed with the Sen2Cor280 tool that generates reflectance values between 0 and 1, corresponding to the wavelengths of the bands (2, 3, 4, 5, 6, 7, 8, 9, 11 and 12).

The 10 bands are stacked into a single raster and resampled with Sen2Res to pixel sizes of 10 m resolution, according to the specifications described in Table 1 (European Space Agency Sentinel).

The mosaic of the pre-processed images is cropped with the shape of the Chira River Basin, as well as the zones identified for the 5 ecological floors.

The spectroradiometer FieldSpec4 was used to measure the spectral signature of the carob tree at three sampling points in the Chira River Basin.

Table 2 shows the climate and geographical location of the three points in UTM coordinates, where a relatively high ambient temperature (TA) is observed, characteristic of a dry forest.

The spectral signature of the carob tree measured with the FieldSpec4 spectroradiometer generates reflectance data between 0 and 1, with a spatial range of 0.001 μm wavelength from 0.35 μm to 2.5 μm (V (0.35–0.7 μm); NIR (0.7–1.0 μm); SWIR 1 (1.0–1.8 μm); SWIR 2 (1.8–2.5 μm)), generating a continuous curve of reflectance values.

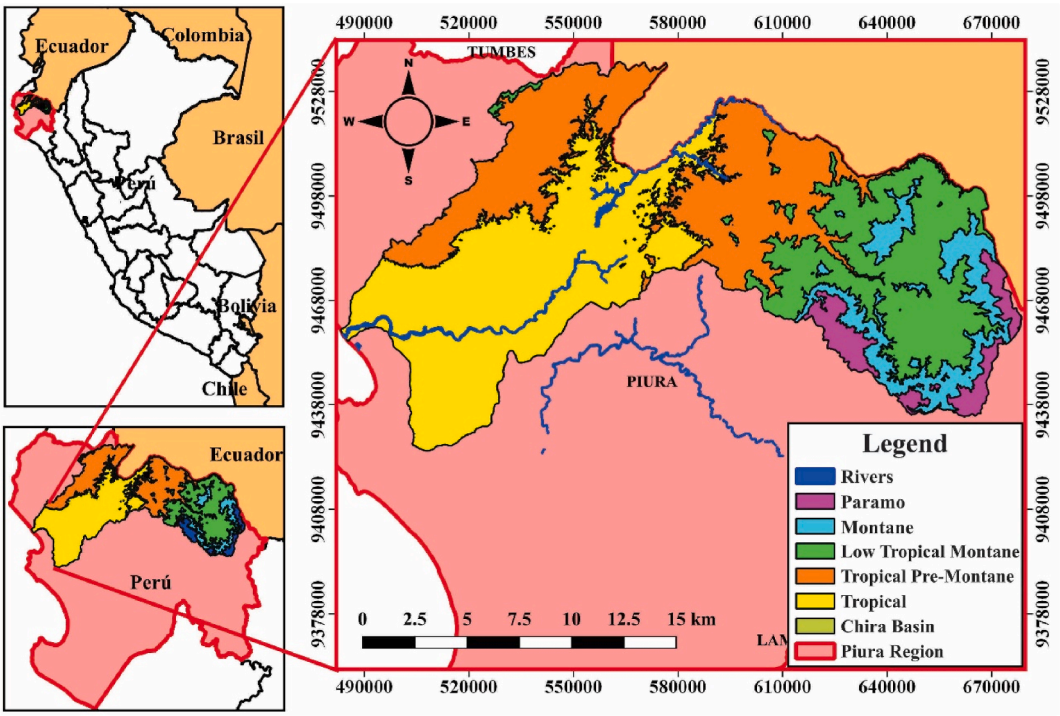

Fig. 1. Geographical location map of the lower Chira River Basin, Piura Region.

Table 1
Spectral description of Sentinel 2 image bands.

Band	Resolution (*m*)	Wavelength (*nm*)	Bandwidth (*nm*)	Description
B01	60	443	20	Ultra blue, coastal and aerosol detection
B02	10	490	65	Blue
B03	10	560	35	Green
B04	10	665	30	Red
B05	20	705	15	VNIR, classifies vegetation
B06	20	740	15	VNIR, classifies vegetation
B07	20	783	20	VNIR, classifies vegetation
B08	10	842	115	Near Infrared
B08A	20	865	20	VNIR, classifies vegetation
B09	60	945	20	SWIR, Water Vapour
B10	60	1375	30	SWIR, Cirrus
B11	20	1610	90	SWIR, discriminates Snow, Ice, Cloud
B12	20	2190	180	SWIR, discriminates Snow, Ice, Cloud

Table 2
Geographical location, in UTM coordinates, of the three carob (*Neltuma piurensis*) sampling points in the Chira River Basin.

Validation Points	Lat.	Long.	Alt. (m)	TA (°C)	Humidity Relative
District Lancones - Sullana	551244	9489275	138	34,0	45
Caserío Cardal - Paimas - Ayabaca	607151	9489939	425	40,0	29
Caserío Macacará - Huaca - Paita	515981	9456565	48	31,6	30

Fig. 2 shows the shape of the spectral signature of the carob tree measured at the sampling points in the sectors of the Macacará hamlet of the Huaca district in the province of Paita (FS4-M), in the Cardal hamlet of the Paimas district in the province of Ayabaca (FS4-C) and in the Lancones district of the province of Sullana (FS4-L) corresponding to the lower basin of the Chira River, their locations in UTM coordinates are described in Table 2.

To identify the spatial coverage of the carob tree in the different ecological zones, the spectral signature of the carob tree from the three sampled points is first imported into the ENVI software, then the Linear Spectral Unmixing tool is used using the Endmember Collection Unmixing option. Subsequently, the desired classification algorithm is chosen.

The procedure involves searching for, locating or recognising the spectral characteristics of the carob tree in the spectral signature as the reflectance values of each wavelength in each pixel corresponding to the 10 bands of the Sentinel 2 image.

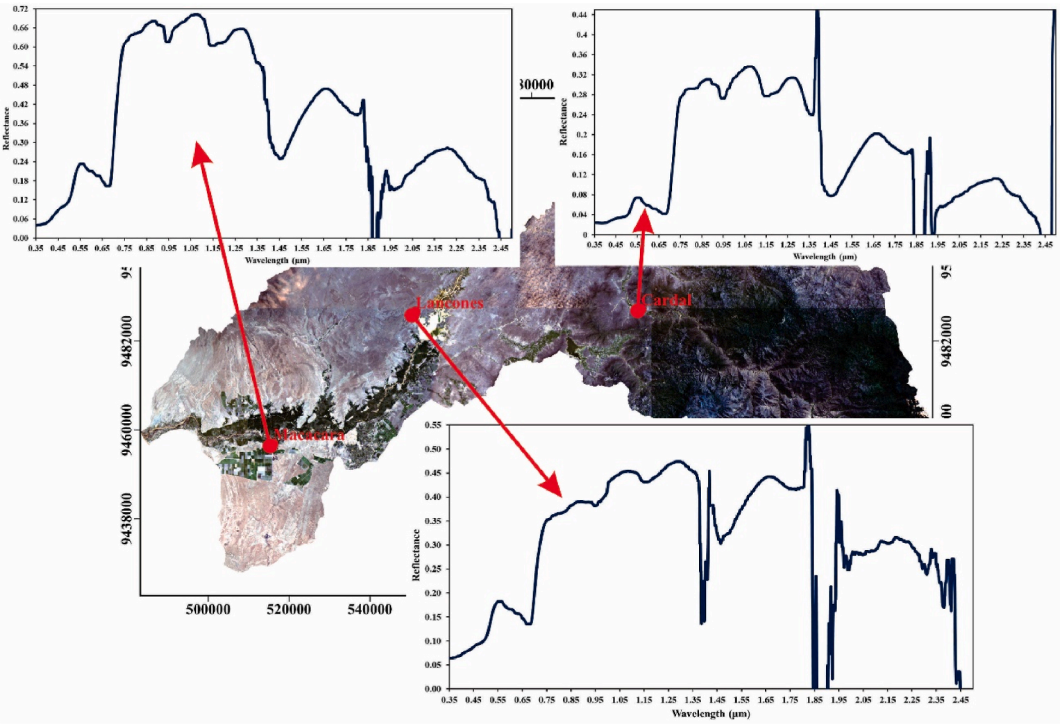

Fig. 2. Sampling points of carob tree spectral signatures, located in Lancones-Sullana; Cardal hamlet of Paimas-Ayabaca and in the Macacará hamlet of the Huaca-Paita, in the Chira River Basin.

Finally, the sampled pixels are counted and multiplied by the size of each pixel (100 m^2) giving rise to the SCCEF of the Chira River Basin.

2.3. Spectral signature of carob (Neltuma piurensis)

The spectral signature of the carob tree shows low reflectance values in the visible spectrum (0.35–0.7 μm), indicating that the absorption of sunlight is dominated by carotenoid pigments (0.48 μm) and chlorophyll an and b which have a characteristic double absorption in the blue and red band (0.45 and 0.67 μm respectively), the green peak (0.55 μm) is the region of the visible spectrum with weak absorption (Chappelle et al., 1992).

However, the near infrared, NIR (0.7–1.3 μm), which is dominated by the air-gap interface of the cell wall due to the structure of the mesophyll or inner tissue of the carob leaf and, to a lesser extent, by discontinuities in the refractive index of the cell constituents, exhibits high reflectivity, which diffuses and scatters energy (Gausman, 1974). The result of the absorbing effect of water where the reflectance is controlled by the water content in the leaves is in the mid-infrared band (1.3–2.5 μm) (Chuvieco, 2008).

In general, the spectral behaviour of carob varies according to phenological changes, whereby the reflectance values of the NIR band are reflected more intensely compared to the other bands. Accordingly, Fig. 3 shows the spectral signatures of the carob tree at three sampling points corresponding to the Lancones, Macacará and Cardal communities, as detailed in Table 2, with differences in reflectance values, but with the same spectral behaviour.

2.4. Ecological levels of the Chira-Piura River Basin

The ecological floor is the geographical area with specific characteristics and patterns of an ecosystem differentiated by the altitudinal floor it occupies. In contrast to (Pulgar and Vidal, 2014) and (Holdridge, 1967), it was found that in the Peruvian territory there are eighty-four life zones and seventeen of a transitional nature, distributed in three latitudinal bands, where a life zone is the vital space that offers the conditions it requires to develop.

However, with the aim of developing an ecological component for the establishment of Life Zones in the Piura Region (Guerra, 2010), the selection of 5 altitudinal or ecological floors in the Piura Region was proposed, based on the criteria of altitude, climate, rainfall, and bioclimatic aspects correlated with vegetation cover. Table 3 shows the SCCEF expressed in km^2 and in percentage with respect to the area established for each ecological floor.

From an ecological point of view, the methodology applied to determine the 5 ecological floors in the continental area (Guerra, 2010; Sisneros et al., 2011), consisted of combining vegetation cover with the sensory and geo-referenced evaluation of 31 Life Zones estimated in the 35892.49 km^2 of the Piura region.

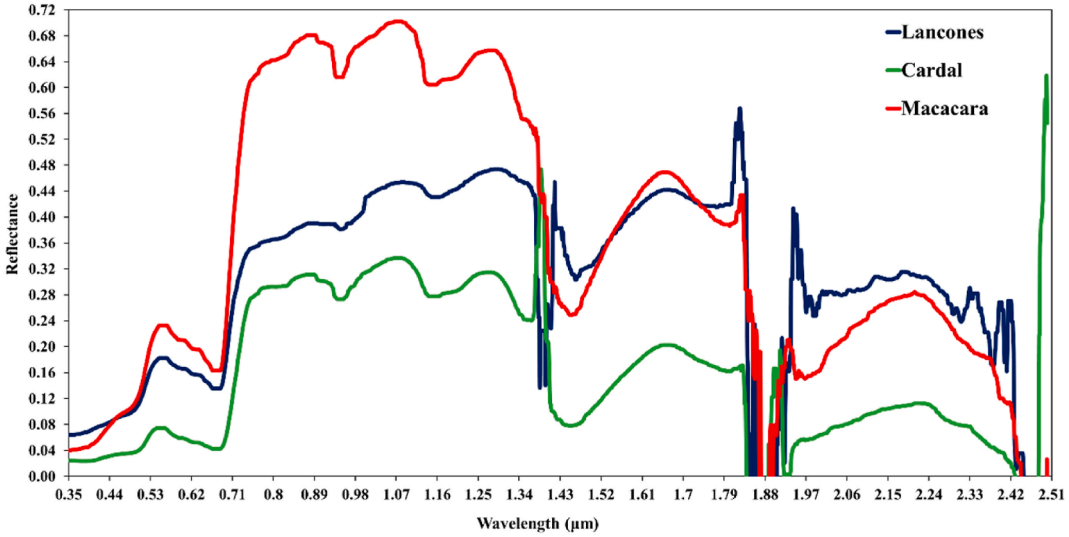

Fig. 3. Spectral signature of the carob tree, measured in Lancones-Sullana; Cardal hamlet of Paimas-Ayabaca and in the Macacará hamlet of the Huaca-Paita.

Table 3
Percentage of spatial coverage of carob tree by ecological floor (%SCCEF) and percentage of spatial coverage of carob tree with respect to the area of the Chira-Piura River Basin (%CEA) in the Piura Region.

N°	Ecological floors[a]	Altitude (masl)	APE (km^2)	CEA (km^2)	%SCCEF	%CEA
1	Tropical (T)	0 a 250	4014.43	62.3634	1.55	0.587
2	Tropical Pre-Montane (TPM)	250 a 1000	3108.94	45.5592	1.47	0.429
3	Low Tropical Montane (LTM)	1000 a 2200	2168.01	16.9163	0.78	0.159
4	Montane (M)	2200 a 3000	860.68	5.9456	0.69	0.056
5	Paramo (P)	>3000	463.83	1.6052	0.35	0.015
Total			10615.89	132.3897	4.84	1.247

[a] Adaptation of the Holdridge Model and life zone studies in the Piura region (Guerra, 2010; Sisneros et al., 2011).

This, based on the distribution of biodiversity developed in the different spaces interrelated with climatic and geographical factors, considering the type of existing flora, adopted from the base of variables worked on and interacted with the thematic of vegetation cover, which in turn supplied the variables of biotemperature and evapotranspiration.

Finally, the necessary information was provided to define the Life Zones with their Ecological Floors, in accordance with Holdridge's Life Zones that provide only a general description of the environmental suitability of the area (Sisneros et al., 2011).

2.5. Application of the Mann-Whitney-Wilcoxon test for the validation of the spectral signature of the carob tree extracted from sentinel 2 images

Mann-Whitney-Wilcoxon *U* test, which identifies a difference between two independent samples with respect to their medians, does not require the sample data to be normal, and it is relatively insensitive to the inhomogeneity of their variance.

If the samples have the same median, each observation will have the same 0.5 (50%) probability of being larger or smaller than the corresponding observation in the other sample. Therefore, the hypotheses are posed.

H0. The two samples of spectral signatures have equal medians.

H1. The two samples of spectral signatures do not have equal medians.

The Mann-Whitney-Wilcoxon $U = min\{U_1, U_2\}$ Mann-Whitney-Wilcoxon test picks out the minimum value from equations (1) and (2) (Yue and Wang, 2002):

$$U_1 = n_1 n_2 + \frac{n_1 (n_1 + 1)}{2} - R_1 \tag{1}$$

$$U_2 = n_1 n_2 + \frac{n_2 (n_2 + 1)}{2} - R_2 \tag{2}$$

where U_1 is the total number of observations of the carob spectral signature extracted from Sentinel 2 images that precede observations of spectral signatures measured with the FieldSpec4 spectroradiometer; U_2 is the total count of observations of spectral signa-

tures measured with the FieldSpec4 spectroradiometer that precede the spectral signature extracted from Sentinel 2 images; n_1 y n_2 are the sizes of both samples; R_1 y R_2 are the rank sums of both samples.

Once the spectral signature of the carob tree extracted from the Sentinel 2 images has been validated, the carob trees are identified in each pixel of a Sentinel 2 image, and then the classified pixels are counted, which, multiplied by the spatial resolution of each pixel (100 m^2), gives the spatial coverage area of the carob tree in each ecological level of the Chira-Piura River Basin.

2.6. Algorithm proposal

The flow diagram in Fig. 4 represents the proposal of an algorithm to determine the SCCEF distributed at different altitudes in the Chira-Piura River Basin.

In a first stage, the spectral signature of the carob tree is measured with the FieldSpec4 spectroradiometer (SSCFS4) in three sample points located in the localities of Lancones, Cardal and Macacará.

The SSCFS4 of each sampled point are correlated with each other to evaluate the strength of consistency between them by means of the coefficient of determination R^2.

In a second stage, Sentinel 2 satellite images are downloaded, then, the spectral signatures of the pixels, corresponding to the bands that make up the Sentinel 2 images (SSCS2), of the three sampled points (Lancones, Cardal and Macacará) are extracted.

The SSCS2 are validated with the SSCFS4 at the three sampled points by applying the U-Mann-Witney-Wilcoxon hypothesis test.

If the validation is significant, the SSCS2 of the three points are introduced in the Sentinel 2 images for the search and characterization of pixels with similar spectral signatures.

Otherwise, other points are sampled to validate the carob tree spectral signatures extracted from the Sentinel 2 images, in those same sampled points.

Once the process is validated, the pixels extracted from the Sentinel 2 images with carob presence by ecological floor are counted.

Finally, the SCCEF is estimated.

- Spatial coverage of carob in the Tropical ecological floor (SCC-TEF).
- Spatial coverage of carob in the Tropical Pre-Montane ecological floor (SCC-TPMEF).
- Spatial coverage of carob in the Low Tropical Montane ecological floor (SCC-LTMEF).
- Spatial coverage of carob in the Montane ecological floor (SCC-MEF).
- Spatial coverage of carob in the Paramo ecological floor (SCC-PEF).

3. Results

3.1. Validation of the spectral signature of carob from sentinel 2 images with the spectral signatures measured with the FieldSpec4 spectroradiometer

The evaluation of the coefficient of determination indicates how similar are the spectral signatures of the carob tree measured in three places of different geographical location (Lancones, Cardal and Macacara) in the Chira-Piura River Basin.

This same spectral response ensures that it is the same plant species (*Neltuma piurensis*) with strong consistency in the visible, NIR and SWIR, in different ecological floors.

Fig. 5 shows that the correlation of the spectral signatures of the carob tree, measured with the FieldSpec4 spectroradiometer, in the localities of Cardal and Lancones have a very high coefficient of determination ($R^2 = 0.972$), of strong consistency in the visible spectrum ($R^2 = 0.967$) and NIR ($R^2 = 0.938$).

The low consistency in SWIR 1 ($R^2 = 0.204$) is due to the water content in the leaves, which absorbs solar radiation at these wavelengths, which is variable between the two sites because they are dry forests with different atmospheric and soil conditions.

Similarly, the correlation between the spectral signatures of the Cardal and Macacará carob trees also have a very high coefficient of determination ($R^2 = 0.993$), with strong consistency in the visible ($R^2 = 0.961$) and NIR ($R^2 = 0.996$) spectra. The high consistency in SWIR 1 ($R^2 = 0.993$) is due to the water content in the leaves, which absorbs solar radiation at these wavelengths, which is the same between both sites with equal atmospheric and soil conditions.

Likewise, the correlation of the spectral signatures of the Lancones and Macacará carob trees has a very high coefficient of determination ($R^2 = 0.973$), of strong consistency in the visible ($R^2 = 0.998$) and NIR ($R^2 = 0.949$) spectra. The low correspondence in SWIR 1 ($R^2 = 0.152$) is due to the water content in the leaves, which absorbs solar radiation at these wavelengths, which is variable between the two sites with different atmospheric and soil conditions.

These high R^2 values between the spectral signatures of the carob trees in the three locations guarantee that the spectral behavior of the carob tree is the same throughout the Chira-Piura River Basin, ensuring greater precision of the algorithm used in the search and identification of carob trees with similar spectral signatures in the pixels of the Sentinel 2 images. Thus, the identification, classification and determination of the spatial coverage of the carob tree in the 5 ecological floors, characteristic of the Chira-Piura River Basin, is significant.

The application of the Mann-Whitney-Wilcoxon *U* test allows the validation of the samples of carob tree spectral signatures extracted from the Sentinel 2 images, from the samples of carob tree spectral signatures measured with the FieldSpec4 spectroradiometer.

Table 4 shows the reflectance values corresponding to the wavelength ranges of the 10 spectral bands of the Sentinel 2 images and those measured with the FieldSpec4 spectroradiometer in the localities of Cardal, Lancones and Macacará in the Chira-Piura River Basin.

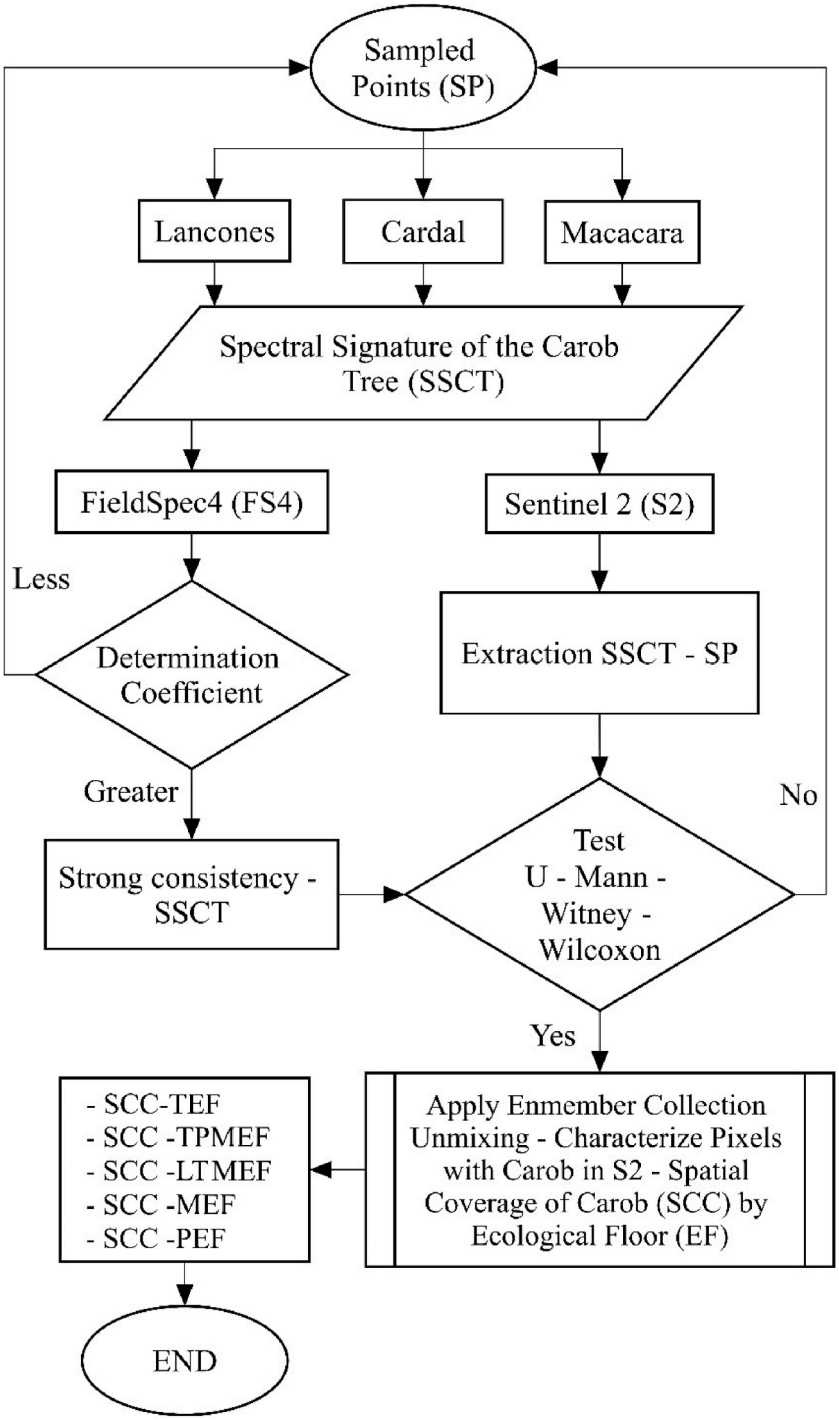

Fig. 4. Flowchart of the algorithm that determines the spatial coverage of the carob tree distributed at different ecological levels in the Chira-Piura River Basin.

The application of the *U* test to the two groups of reflectance values of the spectral signatures at the Lancones location gives a p-value = 0.9705, which is greater than the significance level $\alpha = 0.05$, so the null hypothesis is not rejected, which means that there is no significant difference between the reflectance values of S2-L and FS4-L.

For the two groups of reflectance values of the spectral signatures in the Cardal hamlet, the *U* test gives a p-value = 0.9819 which is greater than the significance level $\alpha = 0.05$, this indicates that these two groups of data do not have significant differences and that both spectral signatures have the same behaviour.

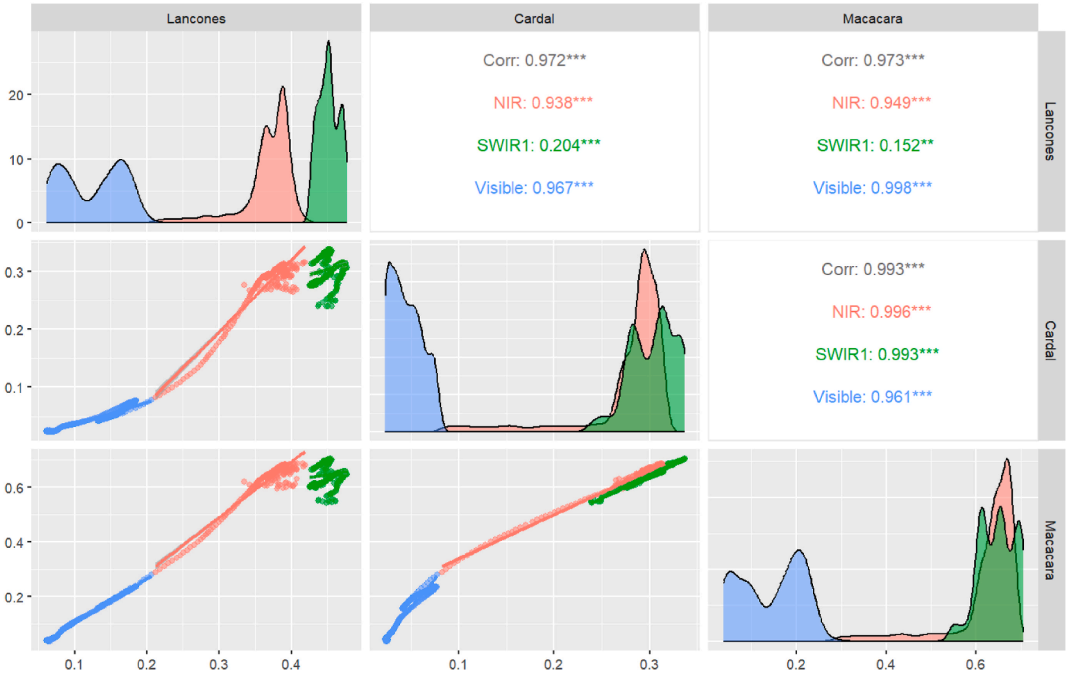

Fig. 5. Correlation of carob tree spectral signatures, measured with the FieldSpec4 spectroradiometer, from the three sampling points located in the localities of Cardal, Lancones and Macacará in the Chira-Piura River Basin.

Table 4
Reflectance values of the spectral signatures measured in the Sentinel 2 image and with the FieldSpec4 spectroradiometer in the localities of Cardal, Lancones and Macacará in the Chira-Piura River Basin.

Band	Wavelength (nm)	District Lancones, Province Sullana		Cardal hamlet. Paimas District. Province of Ayabaca		Macacará hamlet. District of La Huaca. Province of Paita	
		S2-L	FS4-L	S2-C	FS4-C	S2-M	FS4-M
B2	490	0,10565555	0,10035499	0,06072963	0,03619068	0,09768889	0,10771355
B3	560	0,18745554	0,18487763	0,08014445	0,07496757	0,20405555	0,23661316
B4	665	0,13566667	0,13573332	0,04581853	0,04225851	0,12378889	0,16321052
B5	705	0,22609764	0,23550368	0,12160232	0,09950719	0,33629793	0,33184943
B6	740	0,33073228	0,34308826	0,24543653	0,25602809	0,53845707	0,58611367
B7	783	0,35254422	0,36237930	0,26370440	0,29217034	0,64599179	0,63867984
B8	842	0,38769999	0,37785369	0,26666667	0,30301383	0,63975555	0,66502075
B9	945	0,39689377	0,38146752	0,27252399	0,27346325	0,54683422	0,60368819
B11	1610	0,42221588	0,42245629	0,20817501	0,18333334	0,38180886	0,44381740
B12	2190	0,33611253	0,32903901	0,17669109	0,10589172	0,27327288	0,28308425

For the Macacará hamlet, the *U* test gives a p-value = 0.7959 greater than the significance level $\alpha = 0.05$, guaranteeing that both groups of spectral signatures have no significant differences. This confirms the fact that both groups of carob tree spectral signatures extracted from the Sentinel 2 images and measured with the spectroradiometer have no significant differences, so the classification of areas with carob tree cover is accurate with 95% confidence.

Fig. 6(a) shows the Tropical (T) ecological floor, which hosts a spatial coverage of carob of 6236.34 ha (62.3634 km^2) equivalent to 1.6 % of the T area.

Fig. 6(b) shows the Tropical Pre-Montane (TPM) ecological floor which hosts a spatial coverage of carob of 4555.92 ha (45.5592 km^2), equivalent to 1.5 % of the TPM area.

Fig. 6(c) shows the Low Tropical Montane (LTM) ecological floor which hosts a spatial coverage of carob of 1691.63 ha (16.9163 km^2) equivalent to 0.78 % of the LTM area.

Fig. 6(d) shows the Montane (M) ecological floor which hosts a spatial coverage of carob of 594.56 ha (5.9456 km^2) equivalent to 0.7% of the area M and Fig. 6(e) shows the Paramo (P) ecological floor which hosts a spatial coverage of carob of 160.52 ha (1.6052 km^2) equivalent to 0.4% of the area P. The data are detailed in Table 3.

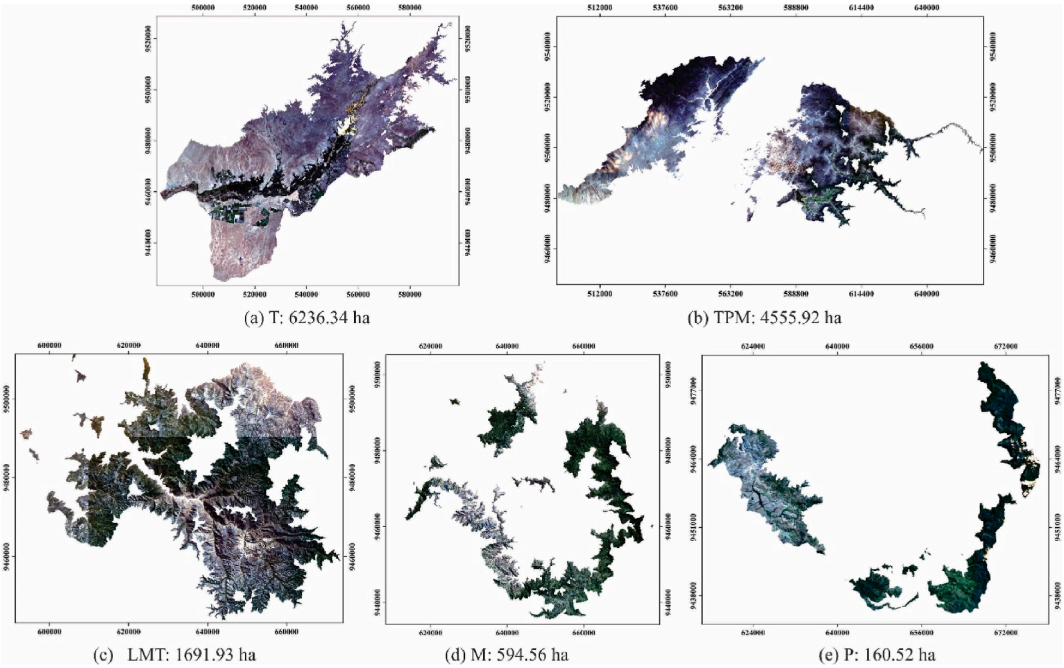

Fig. 6. Spatial coverage of carob by ecological floor in the Chira-Piura River Basin: (a) Tropical (T); (b) Tropical Pre-Montane (TPM); (c) Low Tropical Montane (LTM); (d) Montane (M) and (e) Paramo (P).

3.2. Spatial coverage of carob in the 5 ecological floors

Fig. 7 shows that the SCCEF decreases as the altitude increases, with the Tropical ecological floor at an average altitude of 125 masl being the area with the highest coverage of carob, as well as having the largest surface area in comparison with the other ecological floors. The Paramo ecological floor is the zone with the lowest carob tree coverage, due to its average altitude of 3500 masl.

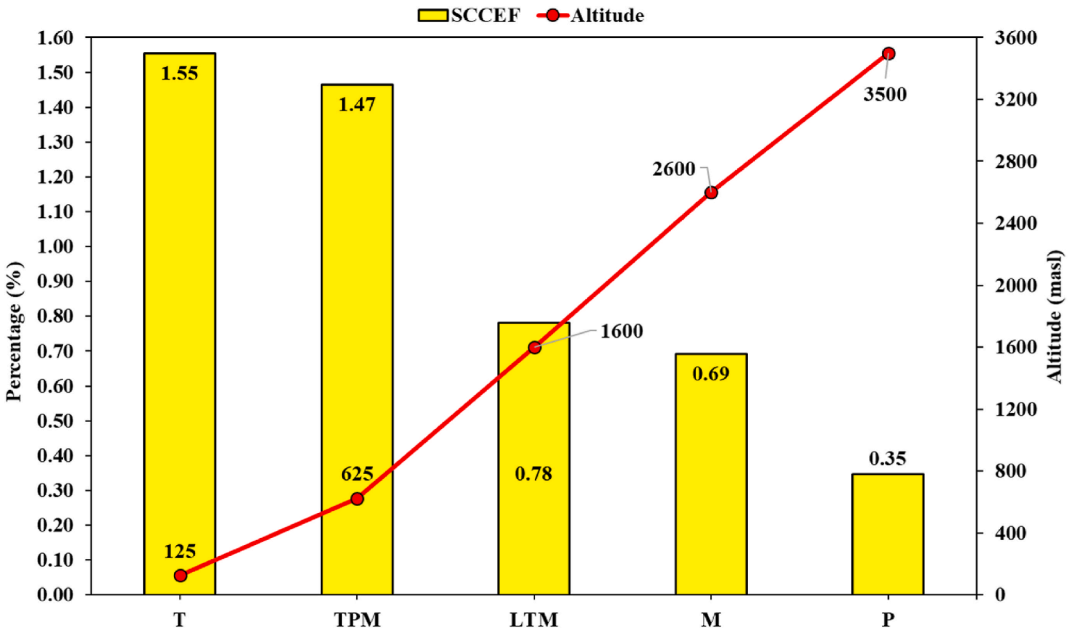

Fig. 7. Spatial distribution of carob trees in the 5 ecological zones of the Chira-Piura River Basin.

4. Discussion

The high correlation between the spectral signatures of the carob trees measured with the FieldSpec4 spectroradiometer in the localities of Lancones, Cardal and Macacará in the Chira-Piura River basin makes it possible to identify the Spatial Coverage of the Carob tree in the Sentinel 2 images in a significant way.

The Spectral Signatures of the Carob trees in the sample points are validated with the spectral signatures of the carob tree measured with the spectroradiometer in the same sample points, by applying the Mann-Whitney-Wilcoxon *U* test, obtaining results similar to those obtained by (Aldana et al., 2020).

Where, the validation was also complemented with the ANOVA test showing that there is no significant difference between the two groups of sampled data.

In this way, it is guaranteed that the identification and classification of carob trees in the different pixels of the Sentinel 2 image are correct with a degree of certainty of 95 %.

It is also ensured that the 5 ecological floors characterised by (Guerra, 2010) in the Chira-Piura River Basin are suitable for the classification of the spatial coverage of the carob tree, demonstrating that at higher altitudes in the Chira river basin there is a significant decrease in the spatial coverage of the carob tree, which, unlike (Salazar et al., 2018), only provides information on the main climatic factors related to the Variability of Intraspecific Traits (VIT) and functional leaf traits of carob at different climatic sites on the Peruvian coast, where it is shown that they follow a decreasing precipitation gradient and an increasing temperature gradient from east to west.

This trend implies that at higher altitudes in the basin, the ecological conditions are not appropriate for the development of the carob tree, considering that at these altitudes the presence of water occurs in greater proportion in all months of the year, however, the climatic conditions (high air and soil temperatures) given in the lower altitude ecological levels generate the appropriate conditions for a good flowering of the carob tree and resilient growth in conditions of water stress, as stated by (Mimbela, 2018).

This confirms the conclusions reached in previous studies by (Padrón et al., 2004b), (Salazar et al., 2023) and (Ambite et al., 2022) that complement the present study as necessary tools for forest management in overexploited arid ecosystems such as the carob tree in dry forest areas and its importance as a major ecosystem service and in hydrology improving soil fertility and moisture, as well as improving desert extremes under its canopy and sustaining the active floodplain (Beresford-Jones et al., 2022).

In general, the northwest coast of Peru is very sensitive to the impact of the ENSO climate phenomenon, which has a strong effect on the growth variability of several dry forest plant species, such as the carob tree, which, according to studies carried out on ring width chronologies, shows clear evidence of the 1997–98 El Niño event (Rodríguez et al., 2005b).

Mapping the location of carob trees at different ecological levels in the Chira-Piura River Basin facilitates the assessment of the intensity of the ENSO event and its impact on the spatial coverage of carob trees, which according to (Salazar et al., 2021b) may be a key species for understanding the resilience of other plants to the ENSO event and the continuous droughts in dry forest ecosystems.

In contrast to (Manaut et al., 2015), the success of reforestation and afforestation strategies with carob trees in dry forests does not only depend on the quality of the seedlings, nor their field conditions, but depends on spatial and temporal monitoring with satellite images of the presence of carob trees at different ecological levels allowing the detection of significant changes in their spatial cover and health status through the measurement of the spectral signature.

The extensive use of carob has an important contribution to the economy of rural communities where the wood is used for housing, cooking, furniture, tools, fodder and medicinal uses, in addition to the industrialization of the fruit.

5. Conclusions

The strong correlation between the spectral signatures of the carob tree sampled in the localities of Cardal, Macacará and Lancones with respect to those measured with the FielSpec4 spectroradiometer, shows that the reflectance values corresponding to the 10 spectral bands behave similarly in the three sectors, inferring correctly in the identification and classification of the areas with carob tree cover in the Sentinel 2 images.

Furthermore, the Mann-Whitney-Wilcoxon *U* test shows that the groups of reflectance values of S2-L and FS4-L (p-value = 0.9705), S2-C and FS4-C (p-value = 0.9819), S2-M and FS4-M (p-value = 0.7959) for the validation points located in Lancones, Cardal and Macacara, respectively, have no significant differences, so that both spectral signatures have the same behaviour. Therefore, it is concluded that the application of the spectral signatures measured with the FieldSpec4 spectroradiometer applied to Sentinel 2 images allows us to accurately characterise the spatial coverage of carob trees in the 5 ecological levels of the Chira-Piura River Basin.

It is shown that the spatial coverage of carob decreases in each ecological floor as altitude increases, so that carob grows abundantly in the Tropical ecological floor (1.6 % of area T) and to a lesser extent above 3500 masl in the Paramo ecological floor (0.4 % of area P), where carob in P does not find the right environmental conditions for its development, so it is inferred that carob grows resiliently in the tropical ecological floor.

It is advisable to carry out future research work focused on the use of artificial intelligence for the detection of areas with carob tree cover or other vegetation species in the forests of the northern coast of Peru that are resilient to extreme climates.

Funding

This research received no external funding.

CRediT authorship contribution statement

Cristhian Aldana: Writing – original draft, Supervision, Investigation, Conceptualization. **Jaime Lloret:** Writing – review & editing, Visualization, Supervision, Investigation. **Wilmer Moncada:** Writing – original draft, Investigation, Formal analysis, Data curation. **Joel Rojas Acuña:** Writing – original draft, Investigation, Data curation. **Yesenia Saavedra:** Validation, Investigation. **Vicente Amirpasha Tirado-Kulieva:** Writing – original draft, Methodology, Investigation, Formal analysis.

Declaration of competing interest

Authors declare no conflict of interest.

Acknowledgments

This work has been possible thanks to the financial support of the Unidad de Proyectos de Investigación de la Universidad Nacional de Frontera; Sullana, Piura, Peru. The authors would like to thank the Laboratorio de Teledetección y energías Renovables LABTELER of the Universidad Nacional de San Cristóbal de Huamanga; Ayacucho, Peru, for their unconditional support for the acquisition of spectral signatures with the FielSpec4 spectroradiometer and the Instituto de Investigación para la Gestión Integrada de Zonas Costeras, Universitat Politecnica de Valencia, Spain.

Data availability

Data will be made available on request.

References

Aldana, C., Revilla, M., Gonzales, J., Saavedra, Y., Moncada, W., Maicelo, J., 2020. Spectral signatures for the identification of dry forest using Sentinel-2 images over the Lower Basin of the Chira river, Piura region. Revista de Teledetección 0, 147–156. https://doi.org/10.4995/raet.2020.14110.

Ambite, S., Ferrero, M.E., Piraino, S., Badagian, J., Muñoz, A.A., Aguilera-Betti, I., Gamazo, P., Roig, F.A., Lucas, C. Prosopis L., 2022. Woody growth in relation to hydrology in south America: a review. Dendrochronologia 76, 126017. https://doi.org/10.1016/j.dendro.2022.126017.

Beresford-Jones, D.G., Whaley, O.Q., 2022. Chapter 7 - Prosopis in the history of the coast of Peru. In: Puppo, M.C., Felker, P. (Eds.), Prosopis as a Heat Tolerant Nitrogen Fixing Desert Food Legume. Academic Press, pp. 95–103. ISBN 978-0-12-823320-7.

Bongers, F.J., Olmo, M., Lopez-Iglesias, B., Anten, N.P.R., Villar, R., 2017. Drought responses, phenotypic plasticity and survival of mediterranean species in two different microclimatic sites. Plant Biol. 19, 386–395. https://doi.org/10.1111/plb.12544.

Borrás, J., Delegido, J., Pezzola, A., Pereira, M., Morassi, G., Camps-Valls, G., 2017. Clasificación de usos del suelo a partir de imágenes Sentinel-2. Rev. Teledetec. 55. https://doi.org/10.4995/raet.2017.7133.

Chappelle, E.W., Kim, M.S., McMurtrey, J.E., 1992. Ratio analysis of reflectance spectra (RARS): an algorithm for the remote estimation of the concentrations of chlorophyll A, chlorophyll B, and carotenoids in soybean leaves. Rem. Sens. Environ. 39, 239–247. https://doi.org/10.1016/0034-4257(92)90089-3.

Chávez, R.O., Clevers, J.G.P.W., Herold, M., Ortiz, M., Acevedo, E., 2013. Modelling the spectral response of the desert tree Prosopis tamarugo to water stress. Int. J. Appl. Earth Obs. Geoinf. 21, 53–65. https://doi.org/10.1016/j.jag.2012.08.013.

Chuvieco, E., 2008. *Teledeteccion Ambiental*; Tercera.; Grupo Planeta (GBS). España. ISBN 978-84-344-8077-3.

Delatorre, J., Pinto, M., Cardemil, L., 2008. Effects of water stress and high temperature on photosynthetic rates of two species of Prosopis. J. Photochem. Photobiol. B Biol. 92, 67–76. https://doi.org/10.1016/j.jphotobiol.2008.04.004.

European space agency sentinel-2. Available online: http://www.esa.int/Our_Activities/Observing_the_Earth/Copernicus/Sentinel-2. (Accessed 8 November 2017).

Gausman, H.W., 1974. Leaf reflectance of near-infrared. In: Photogrammetric Engineering, vol. 40, pp. 183–191. U.S. Dept. of Agriculture: Weslaco. Texas.

Guerra, E., 2010. *Memoria descriptiva para las zonas de vida, pisos altitudinales y biodiversidad en la Región Piura*; Ministerio del Ambiente: Piura. p. 54.

Holdridge, L.R., 1967. Life zone ecology. Life zone ecology.

Holmgren, M., López, B.C., Gutiérrez, J.R., Squeo, F.A., 2006. Herbivory and plant growth rate determine the success of El Niño southern oscillation-driven tree establishment in semiarid south America. Global Change Biol. 12, 2263–2271. https://doi.org/10.1111/j.1365-2486.2006.01261.x.

Hughes, C.E., Ringelberg, J.J., Lewis, G.P., Catalano, S.A., 2022. Disintegration of the genus Prosopis L. (Leguminosae, caesalpinioideae, mimosoid clade). PhytoKeys 205, 147–189. https://doi.org/10.3897/phytokeys.205.75379.

INRENA *Mapa de bosques secos del departamento de Piura : memoria Descriptiva*; Proyecto Algarrobo-INRENA, INR, DGEP, 2003. p. 86. Lima Perú.

La Torre-Cuadros, M., Linares-Palomino, R., 2008. Mapas y clasificación de vegetación en ecosistemas estacionales: un análisis cuantitativo de los bosques secos de Piura. Rev. Peru. Biol. 15, 31–42. https://doi.org/10.15381/rpb.v15i1.1668.

López, B.C., Sabaté, S., Gracia, C.A., Rodríguez, R., 2005. Wood anatomy, description of annual rings, and responses to ENSO events of Prosopis pallida H.B.K., a widespread woody plant of arid and semi-arid lands of Latin America. J. Arid Environ. 61, 541–554. https://doi.org/10.1016/j.jaridenv.2004.10.008.

Manaut, N., Sanguin, H., Ouahmane, L., Bressan, M., Thioulouse, J., Baudoin, E., Galiana, A., Hafidi, M., Prin, Y., Duponnois, R., 2015. Potentialities of ecological engineering strategy based on native arbuscular mycorrhizal community for improving afforestation programs with carob trees in degraded environments. Ecol. Eng. 79, 113–119. https://doi.org/10.1016/j.ecoleng.2015.03.007.

Marmillon, E., 1986. Management of algarrobo (Prosopis alba, P. Chilensis, P. Flexuosa, and P. Nigra) in the semiarid regions of Argentina. For. Ecol. Manag. 16, 33–40. https://doi.org/10.1016/0378-1127(86)90005-8.

Mimbela, N.D., 2018. Influencia de la Temperatura en la Floración del Algarrobo (Prosopis pallida) en los valles: Bajo Piura, Chira. Región Piura-Perú. Revista ECIPerú 14, 10. https://doi.org/10.33017/RevECIPeru2017.0006/.

Padrón, E., Navarro, R.M., 2004a. Estimation of above-ground biomass in naturally occurring populations of Prosopis pallida (H. & B. Ex. Willd.) H.B.K. In the north of Peru. J. Arid Environ. 56, 283–292. https://doi.org/10.1016/S0140-1963(03)00055-7.

Padrón, E., Navarro, R.M., 2004b. Estimation of above-ground biomass in naturally occurring populations of Prosopis pallida (H. & B. Ex. Willd.) H.B.K. In the north of Peru. J. Arid Environ. 56, 283–292. https://doi.org/10.1016/S0140-1963(03)00055-7.

Pulgar Vidal, J.P., 2014. Las ocho regiones naturales del Perú. Terra Brasilis (Nova Série). Revista da Rede Brasileira de História da Geografia e Geografia Histórica 17. https://doi.org/10.4000/terrabrasilis.1027.

Richter, M., Ise, M., 2005. Monitoring plant development after El Niño 1997/98 in northwestern perú. Erdkunde 59, 136–155. https://doi.org/10.3112/erdkunde.2005.02.05.

Rodríguez, R., Mabres, A., Luckman, B., Evans, M., Masiokas, M., Ektvedt, T.M., 2005a. "El Niño" events recorded in dry-forest species of the lowlands of northwest Peru. Dendrochronologia 22, 181–186. https://doi.org/10.1016/j.dendro.2005.05.002.

Rodríguez, R., Mabres, A., Luckman, B., Evans, M., Masiokas, M., Ektvedt, T.M., 2005b. "El Niño" events recorded in dry-forest species of the lowlands of northwest Peru. Dendrochronologia 22, 181–186. https://doi.org/10.1016/j.dendro.2005.05.002.

Salazar, P.C., Navarro-Cerrillo, R.M., Cruz, G., Villar, R., 2018. Intraspecific leaf functional trait variability of eight Prosopis pallida tree populations along a climatic

gradient of the dry forests of northern Peru. J. Arid Environ. 152, 12–20. https://doi.org/10.1016/j.jaridenv.2018.01.010.
Salazar Zarzosa, P., Mendieta-Leiva, G., Navarro-Cerrillo, R.M., Cruz, G., Grados, N., Villar, R., 2021a. An ecological overview of Prosopis pallida, one of the most adapted dryland species to extreme climate events. J. Arid Environ. 193, 104576. https://doi.org/10.1016/j.jaridenv.2021.104576.
Salazar Zarzosa, P., Mendieta-Leiva, G., Navarro-Cerrillo, R.M., Cruz, G., Grados, N., Villar, R., 2021b. An ecological overview of Prosopis pallida, one of the most adapted dryland species to extreme climate events. J. Arid Environ. 193, 104576. https://doi.org/10.1016/j.jaridenv.2021.104576.
Salazar Zarzosa, P., Navarro-Cerrillo, R.M., Palacios Mc Cubbin, E., Cruz, G., Lopez, M., 2023. Biomass estimation models for four priority Prosopis species: tools required for forestry management in overexploited arid ecosystems. J. Arid Environ. 209, 104904. https://doi.org/10.1016/j.jaridenv.2022.104904.
Sisneros, R., Huang, J., Ostrouchov, G., Hoffman, F., 2011. Visualizing life zone boundary sensitivities across climate models and temporal spans. Procedia Comput. Sci. 4, 1582–1591. https://doi.org/10.1016/j.procs.2011.04.171.
Varona, M., 2018. Modelo hidrológico de la cuenca Catamayo-Chira hasta el ingreso al reservorio Poechos usando Hec-Hms. Pregrado, Universidad de Piura: Piura.
Yue, S., Wang, C., 2002. The influence of serial correlation on the mann–whitney test for detecting a shift in median. Adv. Water Resour. 25, 325–333. https://doi.org/10.1016/S0309-1708(01)00049-5.